

Synthesis of Nitrogen-doped Nb₂O₅ for Energy Application



IISER PUNE

A Thesis submitted to

Indian Institute of Science Education and Research Pune

in partial fulfilment of the requirements for the

BS-MS Dual Degree Programme

By

Mr. Naman Kalra

Registration Number: 20141074

Supervisor: **Dr. Bharat B. Kale,**

Director,

Centre for Materials for Electronics Technology (C-MET), Pune.

March, 2019

©Naman

All rights reserved

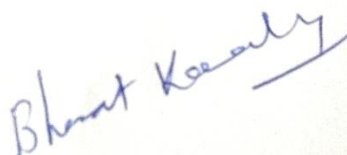
Certificate

This is to certify that this dissertation entitled “**Synthesis for Nitrogen-doped Nb₂O₅ for energy application**” towards the partial fulfilment of the BS-MS dual degree programme at the Indian Institute of Science Education and Research, Pune represents project carried out by “**Naman Kalra** under the supervision of “**Dr. Bharat B. Kale, Director, Centre for Materials for Electronics Technology (C-MET)**” during the academic year 2018-2019.



Signature:

Date: 29 March



Dr. Bharat B. Kale,
Director
C-MET Pune

Declaration

I hereby declare that the matter embodied in the report entitled “**Synthesis for Nitrogen-doped Nb₂O₅ for energy application**” are the results of the work carried out by me at the **C-MET PUNE**, under the supervision of **Dr. Bharat B. Kale** and the same has not been submitted elsewhere for any other degree.



Naman Kalra
(Reg. No.20141074)

Acknowledgements

I would like to express my heartfelt gratitude and sincere indebtedness to my supervisor **Dr. Bharat B. Kale**, Director, C-MET Pune for giving me this stupendous opportunity of doing the thesis project with him. His guidance and motivation whenever I needed it throughout the project had helped me to move in the right direction. I am able to complete this project because of his supervision.

My exceptional much gratitude goes to director Prof Jayant B. Udgaonkar for giving a chance to completing this exploration work.

I would like thank specially to **Rajendra Pamnand, Yogesh Sethi and** who helped me a lot throughout the project. I am also grateful to **Pournima patil,**

Reshma Ballal, Neha Joshi, Soumya kriti, Vijay Autade, and all other members who advised me in the project.

Finally, I want to thank my family for providing me with continuous support and encouragement throughout my years of study.

Table of Content

Abstract.....	10
1. Introduction	11
1.1 Battery	
1.2 Capacitor	
1.3 Super capacitor	
1.4 Nitrogen-doped Nb ₂ O ₅	
2. Experimental Section.....	17
2.1 Techniques for synthesis of Nb ₂ O ₅	
2.1.1 Solid-Solid Combustion	
2.1.2 Sol-gel Process	
2.1.3 Preliminary Trials	
2.2 Characterization techniques	
2.2.1 X-Ray Diffraction	
2.2.2 Ultra-violet visible spectroscopy	
2.2.3 FE-SEM	
2.2.4 Preparation of working electrodes for electrochemical characterization	
2.2.5 Cyclic Voltammetry	
2.2.6 Galvanostatic Charge Discharge	
2.2.7 Electrochemical Impedance Spectroscopy	
3. Result and Discussion.....	23
3.1 Structural Study	
3.2 Surface and Morphology Studies	
3.3 Diffuse reflectance UV-Visible spectroscopy	
3.3 Electrochemical Characterization	

4. Conclusions33

References 34

List of Figures

1. Introduction

Label	Title	Page
Figure 1.1	Scheme of (a) Zinc carbon battery (b) Li-ion battery	12
Figure 1.2	Scheme of (a) electrochemical double layer capacitors and (b) pseudo capacitor	13
Figure 1.3	Ragone plot	14
Figure 1.4	Schematic diagrams of the different faradic processes that give rise to pseudocapacitance.	15

2. Experimental Section

Figure 2.1	<i>Instrumentation of UC-Visible spectrometer</i>	19
Figure 2.2	Scheme Cyclic voltammogram	21

3. Results and Discussion

Figure3.1	XRD patterns of the samples.	24
Figure 3.2.1	FE-SEM images N-Nb ₂ O ₅ at different scale: Sol-gel Process Melamine Percentage (a1, a2- 2.5% b1,b2-5% c1,c2-7.5% d1, d2-10% e1, e2-12.5% and f1,f2-15%)	25
Figure 3.2.2	FE-SEM images of nitrogen doped Nb ₂ O ₅ : Solid-Solid combustion	26

Figure3.3	Diffuse reflectance UV-Visible absorbance spectra of Sol-Gel process and Solid-solid combustion process	27
Figure 3.4.1	N-Nb ₂ O ₅ curves (a) CV at Various scan rate (b) CD at Various current density	27
Figure 3.4.2	N-Nb ₂ O ₅ curves (a) CV at Various scan rate (b) CD at Various current density	27
Figure 3.4.3	N-Nb ₂ O ₅ curves (a) CV at Various scan rate (b) CD at Various current density	28
Figure 3.4.4	N-Nb ₂ O ₅ curves (a) CV at Various scan rate (b) CD at Various current density	28
Figure 3.4.5	N-Nb ₂ O ₅ curves (a) CV at Various scan rate (b) CD at Various current density	28

Figure3.4.6	N-Nb ₂ O ₅ curves at Various percentage (a) CV at 10 mVs (b) Nyquist Plot(c) Rate Capability (d) Specific Capacitance Vs Scan rate	30
Figure 3.4.7	CV curves at Various scan rate for (a) N-NbO-6, (b) N-NbO-10 and (c) N-NbO-15	31
Figure3.4.8	Nitrogen doped Nb ₂ O ₅ (a) Nyquist plot (b) Specific capacitance vs scan rate (c) CV at 10mVs	32

ABSTRACT

Recently metal oxide based supercapacitor has immense importance due to their enhanced capacitive properties. Niobium Oxide (Nb_2O_5) as a metal oxide can be useful due to its availability, economic and environment factors, but its use in the application of energy storage and devices is very limited. In this thesis, we have Nitrogen-doped Nb_2O_5 (N-doped Nb_2O_5) which is synthesized through solid combustion and sol-gel method and their application in terms of supercapacitive performance are measured

Proper doping of nitrogen doped Nb_2O_5 into activated carbon enhances its super capacitive properties. Nitrogen doping shows very interesting and encouraging results but it has not been studied by many researchers. However, detail study with varying percent doping has to be explored. Hence, in the present work, the nitrogen doped Nb_2O_5 will be synthesized and characterized with different techniques for its phase purity and electrical properties. Further, the electrochemical / super capacitive performance will be demonstrated with respect to N doping in Nb_2O_5 . After that material characterization (SEM/XRD//Edax etc.) and device characterization (CV/impedance/cyclic stability etc.) will be performed to check the properties and performance of synthesized material and fabricated supercapacitor.

1. INTRODUCTION

In recent times, energy storage and conservation has been attracting everyone's sight due to the increasing energy, environment and its effects, and continuous depletion of natural resources [1-5]. Energy storage is one of the greatest challenges of the 21st century in science and research department, stirred by the growing demand for renewable but irregular energy supplies and mobile power sources [6]. Among storage processes, electrochemical energy storage is considered for most number of uses. Electrochemical energy production can be considered as an extra power source, as long as this energy is more economic and sustainable. The different types of Systems for energy storage include batteries, electrochemical capacitors (ECs), and fuel cells. We can see the energy storage and their conversion processes are different, there is "electrochemical similarities" of these three mentioned systems. Common functions include the energy generation processes taking place at the surface of the electrode and electrolyte medium and the transport of electrons and ions are separated [7]. In comparison to all these devices, batteries have fetched by far the dominant position due to covering the most number of applications, Whereas supercapacitors have found their use in the electronics markets. Therefore, zero emission electrochemical conversion devices and storage devices such as batteries, capacitors and fuel cells are suitable alternatives to address the existing calamities. Although these technologies have different ways to store and convert energy, but they are common in the energy giving process that occurs at the electrode-electrolyte interface.

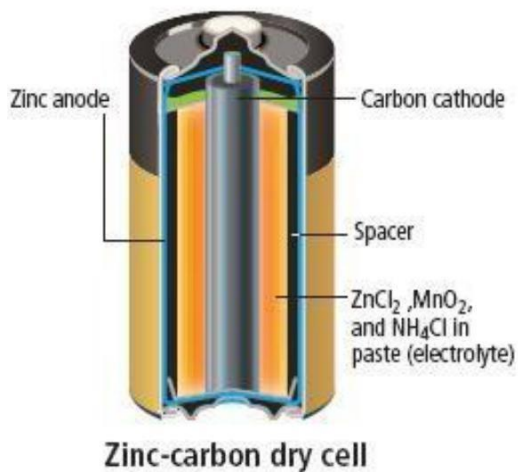
1.1 Battery

Battery can be termed as the electrical connection of one or more electrochemical cells. A battery basically consists of anode also called positive electrode and cathode also called negative electrode separated by electrolyte solution. Charge transfer reactions that is happening near the electrode/electrolyte boundary leads to a potential difference between the anode and cathode. [8] Due to these potential

difference, there is flow of electrons from electrode having low reduction potential to the electrode having relatively high reduction potential. So, this results in cell the conversion of chemical to electrical energy during charge discharge phenomenon .^[9]

Battery can be viewed as basically a chemical energy storage device which results in conversion into electrical energy only when it is required. There are several categories such as Primary battery and secondary battery are two different categories of battery. Primary battery is the no chargeable battery whereas secondary battery is chargeable battery^[9]. Examples of primary batteries include alkaline battery and zinc carbon. Nickel metal battery, Lithium-ion battery and lead battery are part of secondary batteries.

a



b

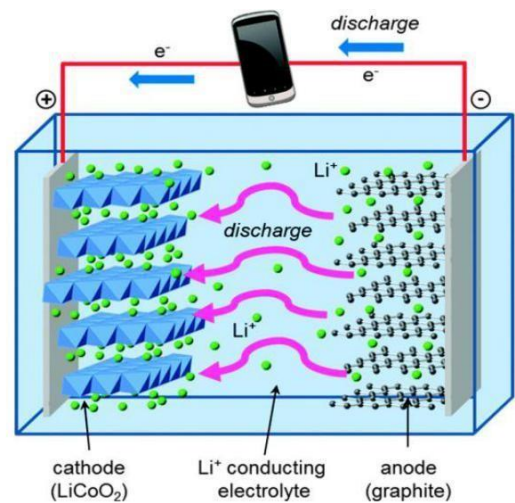


Figure 1.1: Schematic of (a) Zinc-carbon battery and (b) Li-ion battery

http://glencoe.mheducation.com/sites/007874637x/student_view0/chapter20/section2/self_check_quizzes.html#quest4

1.2 Capacitor

Capacitors are made up of electrodes and are separated by dielectric which acts as insulating material. Capacitors in basic terms use stored charge rather than chemical process to store energy. When a voltage is given across the capacitor, opposite charges accumulate and concentrate on the surface of both the electrodes. These charges are kept separated by the use of dielectric, thus leading to creation of induced electric field that results in storage of energy in capacitor in terms of charge.^[9]

1.3 Supercapacitors

Supercapacitors are different from simple capacitors in two ways; its surfaces have a larger surface area and the distance between the plates is smaller, while the separator between the plates in supercapacitors works differently than the dielectric in a capacitor. The capacitor plates are separated by dielectric but in a supercapacitor there is no dielectric. Instead, both these conducting plates are immersed in electrolyte which are separated by an insulator^[10]. Therefore supercapacitors (SCs) are important energy storage devices with high energy and power density compared to capacitors and batteries as seen in Ragone plots^[11,12]. The two different types of electrochemical supercapacitor are electrochemical double layer capacitors (EDLC) and pseudo capacitors. In EDLC the storage of charges happens due to the ion adsorption at the electrode/electrolyte boundary and for pseudo capacitors charge storage happens due to redox reaction at the surface.^[10,13]

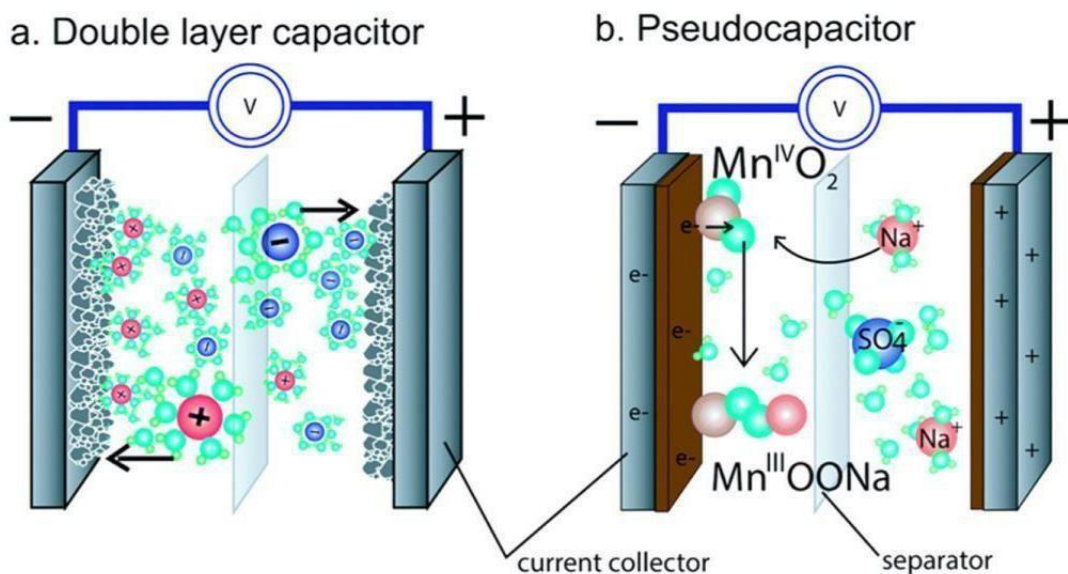


Figure 1.2: Scheme of (a) electrochemical double layer capacitors and (b) pseudo capacitor

<http://iopscience.iop.org/article/10.1088/0957-4484/27/44/442001>

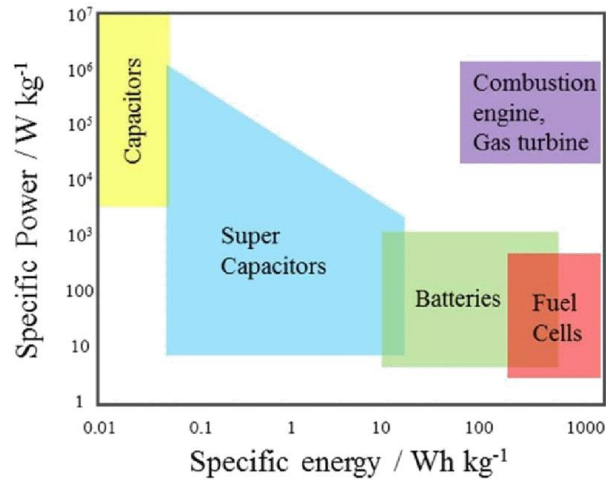


Figure 1.3. Ragone plot for different storage devices.

https://www.researchgate.net/profile/Myounghoon_Choun/publication/316605004

From the above plot, comparing the batteries and supercapacitors, the latter shows higher values of power density and low energy density. Hence, working on the development of supercapacitors by improving its energy density has become the topic of wide attraction.

As mentioned above, Supercapacitors are of two categories, Pseudocapacitor which stores charge electrochemically and EDLC which stores charge electrostatically. In terms of working of a Pseudocapacitor, three different mechanisms can be observed: Underpotential Deposition, Redox pseudocapacitance^[16,13] and intercalation^[17].

pseudocapacitance. The three different mechanisms lead to the contribution of the total pseudo capacitance obtained. In Underpotential Deposition electrostatic surface charging occurs where the mobility of these ions is controlled by the electrolyte which affects the ionic conductivity. [14, 15] Charge accumulation results in reduction in capacity leading to a low energy density. It has good cycle stability due to the absence of electrode degradation by redox reactions. The material which is able to show different or multiple oxidation states in range of voltage window of the electrolyte chosen as reactions occur and it exhibits greater capacity due to the transfer of electron across the electrolyte boundary

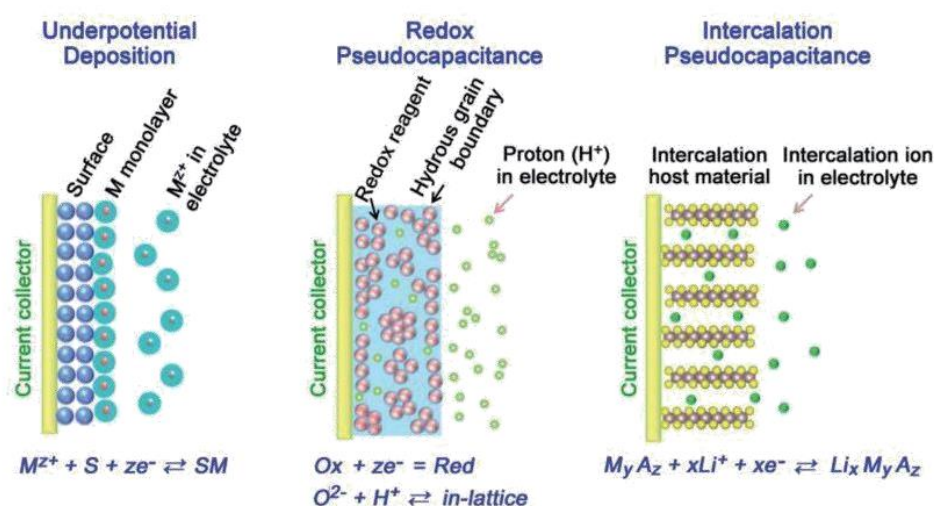


Figure 1.4 Schematic diagrams of the different faradic processes that give rise to pseudocapacitance.

<https://onlinelibrary.wiley.com/doi/pdf/10.1002/advs.201700322/Figure4>.

The third mechanism is intercalation and in this positive ions are diffused deeper into the electrode framework which allows more of them to diffuse resulting larger storage of charges. The diffusion length of cations can lead to the efficiency change. Diffusion length is explained by the electrode arrangement. Smaller the diffusion length faster will be the reaction. Nanostructures reduce diffusion length leading to more charge intake^[18]. This process is relatively slow in occurrence because ions have to cover a distance to get diffused and also due to the higher resistance encountered in an electrode structure. As a consequence of this, the charge/discharge rates gets low. The first two mechanisms occur at the surface and ensure a fast charge/discharge rate.

1.4 Nitrogen-doped Nb₂O₅

Niobium Pentoxide (Nb₂O₅) with a low band gap of around 3.4eV which is low compared to other electrolytes, is n-type semiconductor. The interest arised in studying of Nb₂O₅ is due to its availability, low cost factor and shows great potential and stability in aqueous medium. Earlier studies have shown use of Nb₂O₅ in photocatalyst in hydrogen generation. Nb₂O₅ shows great potential and stability due to thermodynamic stability, its surface acidity, redox and photocatalytic properties due to the structure of Nb₂O₅. Therefore it acts as good photocatalyst for hydrogen generation.

Nitrogen doped Nb₂O₅ is proved to be a good anode material for lithium-ion battery. It acts as good photocatalyst for hydrogen generation. It is a good x-ray absorber and radiation shielding material and will be stable material for supercapacitor due to its abundance, high surface area, and porous structure, and suitable electronic structure, good optical and electronic properties.

The nitrogen-doped graphene has shown the enhanced performance for lithium ion battery and other energy storage devices. Therefore, nitrogen doped Nb₂O₅ could be expected to show the enhanced performance for supercapacitors.

2. EXPERIMENTAL SECTION

2.1 Experimental Section

2.1.1 Synthesis of Nitrogen-doped Nb₂O₅ –Solid-Solid combustion process.

Nitrogen doped Nb₂O₅ is synthesized by solid-solid combustion reaction process. We have made sure the Analytical use of chemicals and without purification. NbCl₅ (Aldrich) is used as a niobium source and urea (Fisher scientific) is added as the nitrogen source. In this type of synthesis, niobium chloride (NbCl₅) and urea (N₂H₄CO) are mixed in mortar pestle for about 20 minutes in the molar ratios of 1:2, 1:6, 1:10 and 1:15, respectively. After this, the homogenous mixture which now appears to be dry jelly is transferred in an alumina crucible and calcinated in furnace for 3h to carry out the reaction. After completion of the reaction process, the resultant product was washed with small amount of distilled water to remove the chlorine. After the washing it was treated with ethanol and kept for drying at 80°C for 24 hours. The synthesis by above procedure is labelled as N-NbO-2 (1:2), N-NbO-6 (1:6), N-NbO-10 (1:10), and N-NbO-15 (1:15).

2.1.2 Synthesis of Nitrogen-doped Nb₂O₅ -Sol-Gel process.

Sol Gel process describes as the wet-chemical technique also called as the chemical solution deposition. The materials synthesized by this sol gel technique can be used and has found applications in energy, electronics, sensors, medicines and space. The rate of hydrolysis and condensation of molecular precursors are major drawback of sol gel. These reactions occur at a very fast rate, which results in loss of structural and morphological control over the oxide materials.

Besides, the difference in reactivity of these oxides makes it difficult to control the uniformity and composition of the metal oxides by this process. Nitrogen doped Nb₂O₅ synthesized by the Sol-gel method. Niobium chloride (0.025M) was used as the starting precursor, citric acid (1M, 100mL) and Melamine(2.5%,5%,7.5%,10%,15%) of NbCl₅ molar concentration were mixed. After thoroughly mixing the mixture was kept for heating at 80°C for 24 hours. Further the dry gel mixture is calcined in electric furnace at 500°C for 2 hours. After the formation of product, the resultant product was cooled to room temperature and the weight of the compound was noted.

a) Preliminary trials

I have tried to prepare Nitrogen doped Nb_2O_5 through solid-solid combustion and sol-gel process. During the solid-solid combustion reaction the homogeneous mixture was heated at 400,500 for 2 h respectively. After going through the XRD of powder at 400 for 2h we observed noise in XRD patterns. This may be due to the amorphous nature of the sample. Hence keeping this in mind I tried to calcinate the sample at 500 for 2h and the XRD patterns were obtained which matched with the reference XRD data.

During the Sol gel process the mixture was heated at 500 for 6h followed by various trials at 600 for 3h. The color of the compound obtained in respective cases was white which indicates there is no presence of nitrogen in the final product. The XRD patterns as well confirmed that the compound which I was aiming for was not synthesized. After going through trials the mixture was heated at 500 for 2h and the color of the compound obtained was a mix of light yellow and black. And after observing the XRD patterns which shows the presence of amorphous nature we calcined the sample again at 500 for 2 hours. After this improvisation we observed the XRD patterns and found that, this matched with the reference sample.

During the synthesis of Nb_2O_5 from above mentioned processes the temperature rate was varied and the atmosphere in which the sample was calcinated was also varied. Keeping in mind all the results that we have got through variation we have synthesized Nitrogen doped Nb_2O_5 successfully.

2.2 Characterization techniques

2.2.1 X-Ray diffraction (XRD)

XRD technique is used for characterization of nanomaterials. It is a nondestructive technique used for detection of crystallinity, crystal structures, and the lattice constant of materials. Each crystalline material gives a specific XRD pattern i.e. the same material always gives the same pattern; and in a mixture, each produces its pattern irrespective of the others. The X-ray diffraction pattern of a pure substance can be consider as “characteristic” of the substance. The crystallinity and phase purity were examined by X-ray diffraction (XRD, Advance, Bruker AXS D8) scanned in the 2θ range from 10 to 80° .

2.2.2 Ultra-violet visible spectroscopy

Optical absorption spectroscopy (UV-Vis. Spectroscopy) is a method to study metals, semiconductors and insulators in bulk, thin film, nanostructures morphologies etc. Semiconductors and insulators shows an optical energy difference. The absorption of the wavelength takes place, when there is sufficient amount of energy to excite the electron from valence band to conduction band. At high energy or short wavelengths, there is continuous absorption of photons. The absorbed (or reflected) intensity as a function of wavelength from ultraviolet (200 nm) to infrared (3000 nm)

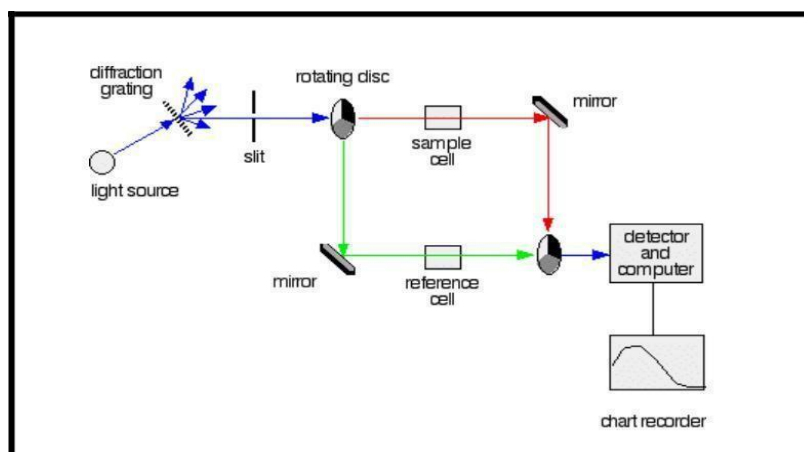


Figure2.1 Instrumentation of UC-Visible spectrometer.

(Picture Credits <https://www.chemguide.co.uk/analysis/uvvisible/spectrometer.html>)

Or many times up to 1000 nm) is used to determine the transitions between conduction and valence band of materials and electronic structures and to determine the electronic structure. With reduction in the particle size, the absorption edge shifts toward lower wavelengths and it is known as blue shift.^[26]

2.2.3 Field Emission Scanning Electron Microscopy (FESEM)

FESEM is used to study the small surface and morphological details of the materials and Objects. In case of FESEM equipment electrons emits from a field emission source and Accelerate in a high electrical field. Electronic lenses focuses the primary electrons in to a Narrow scan beam that bombards the object. The secondary electrons are emits from object surface due to bombardment. The angle and velocity of these secondary electrons plays the crucial role to get the surface structure and morphology of the object. Electronic signal is produced by the detector by detecting the secondary electron emitted from the material. This signal is amplified and converted to image on a monitor processed further. Morphological studies were performed with Field Emission Scanning Electron Microscopy (FESEM, Hitachi S-4800).

2.2.4 Preparation of working electrodes for electrochemical characterization

Working electrodes, for electrochemical studies of the synthesied samples were prepared by taking 8:1:1 as of synthesized material, carbon black, and PVDF binder respectively using solvent N-methyl-2- pyrrolidinone (NMP).The above mixture was grinded and uniform slurry was prepared and then it was coated uniformly on the Toray Carbon electrode. The weight of the Toray carbon paper was noted before and after coating. The Toray carbon paper was dried overnight in an oven at 100^oC before and after coating for testing. The electrochemical measurements were conducted in an essential medium using 1M Na₂SO₄ as an electrolyte for GCD, CV, EIS using a three electrode system for Pseudocapacitor, where the Platinum electrode was used as a counter electrode with Ag/AgCl and Hg/HgO as a reference electrode.

2.2.5 Cyclic voltammetry (CV)

Cyclic voltammetry is the technique used for studying electrochemical reaction mechanism i.e., redox reaction mechanisms occurring in electrochemical analysis. In a cyclic voltammetric experiment, the working electrode is scanned linearly from an initial applied voltage E1 to a final switching voltage E2 at which the direction of the scan is reversed. The applied voltage is known as the scan rate which means that during the experiment the potential varies linearly at that speed. The current is plotted as a function of applied voltage. The peaks in a CV diagram represents redox processes.

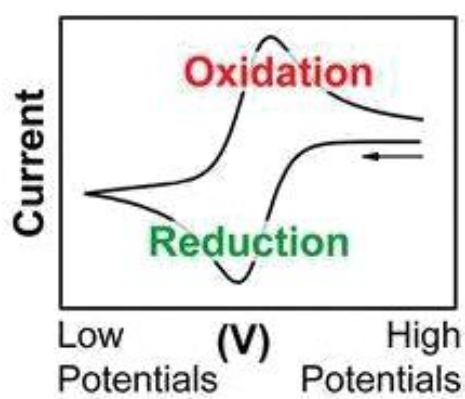


Figure 2.2 Scheme Cyclic voltammogram

During the negative scan, the analyte undergoes reduction, and the corresponding current is known as cathodic current same when the scan is in a positive direction, the oxidation of the analyte occurs, and the current corresponding to the oxidation peak is called anodic current. The specific capacitance from CV is calculated by the given formula

$$C = \frac{\int I \cdot \Delta v}{v \cdot m \cdot \Delta V}$$

whereas, \int denoted negative current swiped area by , Δ is potential window , m is electroactive material mass, v is scan rate. In a three-electrode system, the potential is measured between the reference and working electrode and the current is measured between the counter and working electrode.

2.2.6. Galvanostatic charge-discharge (GCD)

Galvanostatic charge-discharge is an electrochemical technique conducted to measure the electrochemical performance and cycle life of batteries and capacitors. In this

technique, the electrode is charged and discharged cyclically. For the analysis a constant current is applied between the reference and working electrode and the potential between the counter and working electrode concerning the reference electrode is measured. Both charging and discharging are conducted at constant current applied until a set voltage is reached. For data analysis, the potential of the electrode is plotted as a function of time concerning a reference electrode.

2.2.7. Electrochemical impedance spectroscopy (EIS)

Impedance can be defined as the measure of the ability to resist the flow of electric current of the circuit. Naturally, it is a tool for the analysis of non-linear electrochemical processes. In the EIS technique, the measurements are made by applying a small sinusoidal potential of fixed frequency, and the response is obtained as a sum of sinusoidal functions. It is capable of delivering information about the diffusion resistance capacitive behaviour of the material and the rate of electron transfer reactions. The data obtained from an EIS technique are represented in a way that the real part is plotted along X-axis and the imaginary part along Y-axis, such plots are referred to as Nyquist plots, and each point present in them represents the impedance at that frequency.

RESULTS AND DISCUSSION

Nitrogen doped Niobium oxide is synthesized varying concentration of melamine in sol-gel process and varying ratio of niobium chloride to urea in solid combustion process. The ratio of niobium chloride to urea was changed from 2, 6, 10 and 15M in solid state combustion and melamine concentration was varied for sol-gel process and results were observed for 2.5%, 5%, 7.5%, 10%, 15% melamine respectively. After the completion of reaction of at 500^o C there is release of ammonia. This released ammonia forms sphere around Nb and acts as the source of nitrogen for this solid state combustion which further penetrates into the lattice structure. because of the calcination at higher temperatures the NbCl₅ leads to Nb₂O₅. The following reaction can be expressed as



As the concentration of urea increases, there is improvement in combustion rate due to increase in combustible gases thus the exothermicity increases linearly with reaction. This is clearly reflected on the morphology, crystallinity and large bulk nitrogen content in Nb₂O_{5-x}N_x with increase in urea amounts.

The melamine is expected here to be main source of nitrogen for sol-gel technique. The calcination at higher temperature leads to formation of Nb₂O₅.

3.1 Structural study

The Study of Fig3.1 which shows XRD of nitrogen doped Nb₂O₅ catalysts obtained from Sol-gel process and solid-solid combustion process having varying ratio of niobium chloride and Urea calcined at 500^oC. We can observe the peaks at 22.3^o, 28.5^o, 36.5^o, 46.3^o, 50.4^o, 55.2^o, 59.1^o, 64.1^o, 70.9^o, and 78.0^o are indexed as (001), (200), (181), (002), (321), (182), (2160), (2161), (382) and (3122) planes, respectively. There is no noise in the diffraction peaks which tells us that there is no formation of oxides other than Nb₂O₅. These intense peaks shows the formation of orthorhombic structure which has the properties of high crystallinity XRD peaks are in match with the reported (JCPDS No. 30-0873) which matches the space group (*Pbam*) having lattice constants a 6.175 Å, b 29.175 Å and c 3.930 Å. The XRD

peaks at 36° and 55° shows the behaviour same as that of orthorhombic ($T\text{-Nb}_2\text{O}_5$). The synthesized samples have crystalline structure which states that N-doping has a no effect on the crystal structure of Nb_2O_5 .

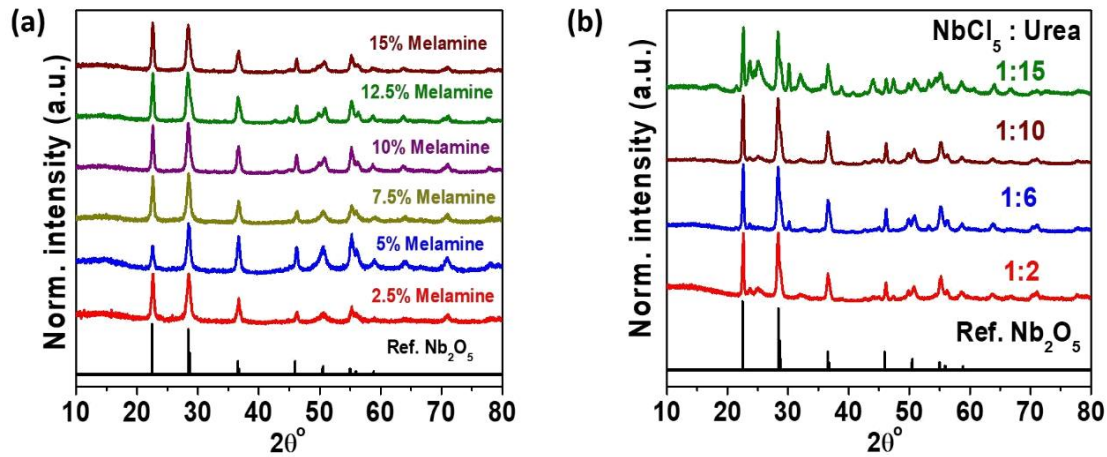


Fig 3.1 XRD patterns a) Sol-gel (b) Solid-Solid combustion.

3.2 FESEM Analysis

Fig. 3.2 (a-f) shows the FESEM images (morphological and structural study) of the as-synthesized N-doped Nb_2O_5 samples through sol-gel process. The surface morphology of the samples shows as we increase the melamine concentration there is formation of better nanocrystals. The uniformity is observed in all of these samples. XRD and FESEM studies

Both FESEM and XRD results show that N-doped Nb_2O_5 possess the same crystalline structure and morphology for the sol-gel process.

Fig. 3.3 (a-d) shows the FESEM images of the synthesized N-doped Nb_2O_5 through solid combustion process for varying ratio of niobium chloride and urea. For the sample NbO-2 (Fig 3.3. a1, a2) the surface morphology describes rod shape morphology at various size lying in the range of 50-100 nm. Fig 3.3 (b1, b2) shows the images of NbO-6 which shows that for this ratio of urea and niobium chloride we observe the mixed morphology in the range nanoparticles of size 50 nm and thin flakes (100 nm). For NbO-10 (Fig 3.3 c1 and c2) here for this ratio it shows interlocked chain like structures which are porous, due to the interlocking thus creating porosity along with it shows the presence of tiny nanoparticles of the size 10-15 nm. The Fig 3.3. (d1 and d2) for the maximum urea concentration it shows the full development of the distorted rectangular shaped rods which are made up of many tiny rods giving the

overall size 1-3 μm . From previous observation due to doping of oxides it does not allow the one-dimensional growth of the nanoparticles as seen in NbO-6 and NbO-10 sample due to limiting the growth of rods. From the FESEM results it is observed that as we increase the ratio of niobium chloride and urea there is a change in morphology of the synthesized samples. Very small nanoparticles with high porosity is observed in the case of NbO-10 because of the adequate exothermicity and further, as we increase the concentration of urea i.e. in the case of NbO-15 the nanorods are formed.

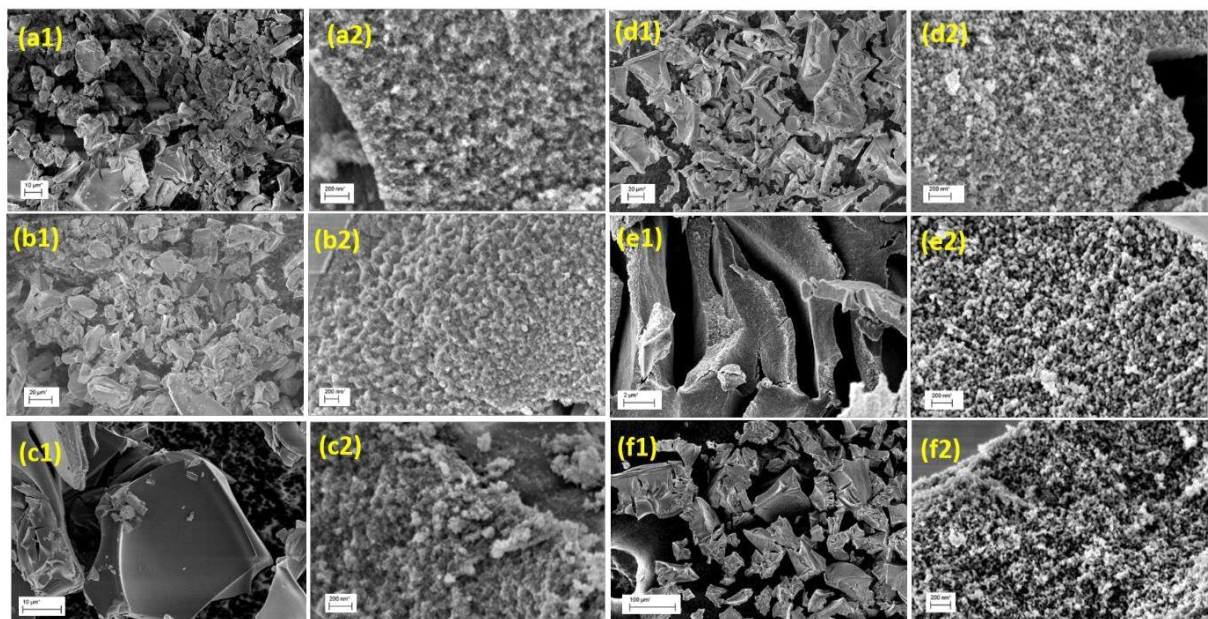


Fig3.2.1 FE-SEM images of nitrogen doped Nb_2O_5 at different scale: Sol-gel Process Melamine Percentage (a1, a2- 2.5% b1,b2-5% c1,c2-7.5% d1, d2-10% e1, e2-12.5% and f1,f2-15%)

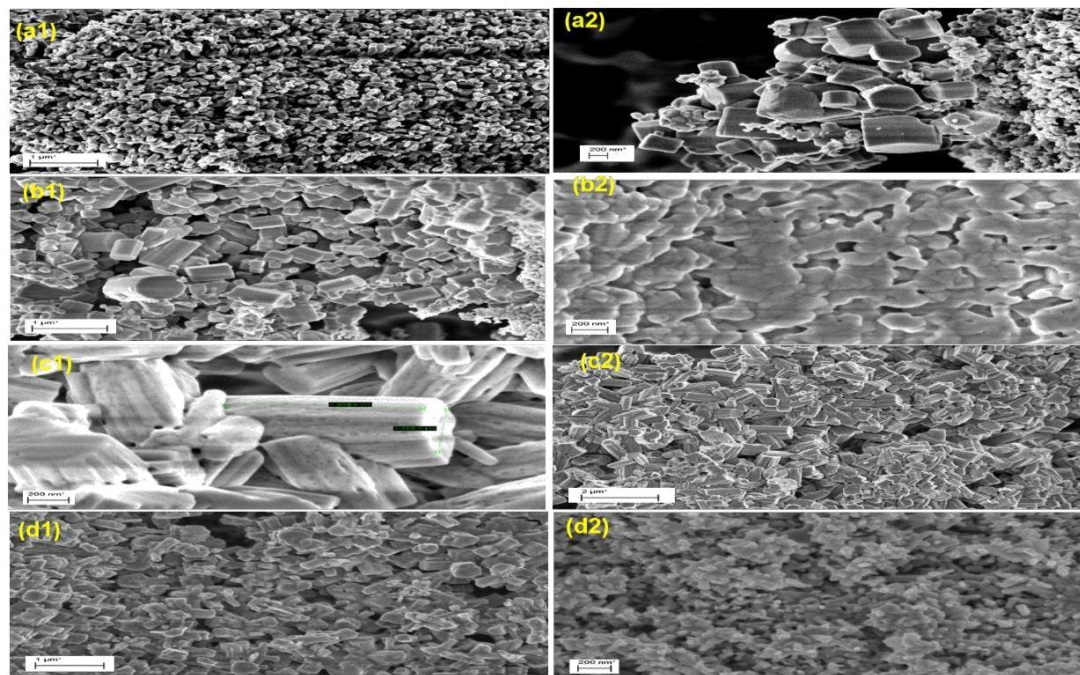


Fig.3.2.2 FE-SEM images of nitrogen doped Nb_2O_5 : Solid-Solid combustion
(a1, a2- N-NbO-2; b1,b2- N-NbO-6; c1,c2- N-NbO-10; d1, d2- N-NbO-1)

3.3 Diffuse reflectance UV-Visible spectroscopy

To study the optical properties of synthesized materials diffuse reflectance UV-Visible spectra is recorded in the range from 200 nm to 800 nm of doped and as synthesized Nb_2O_5

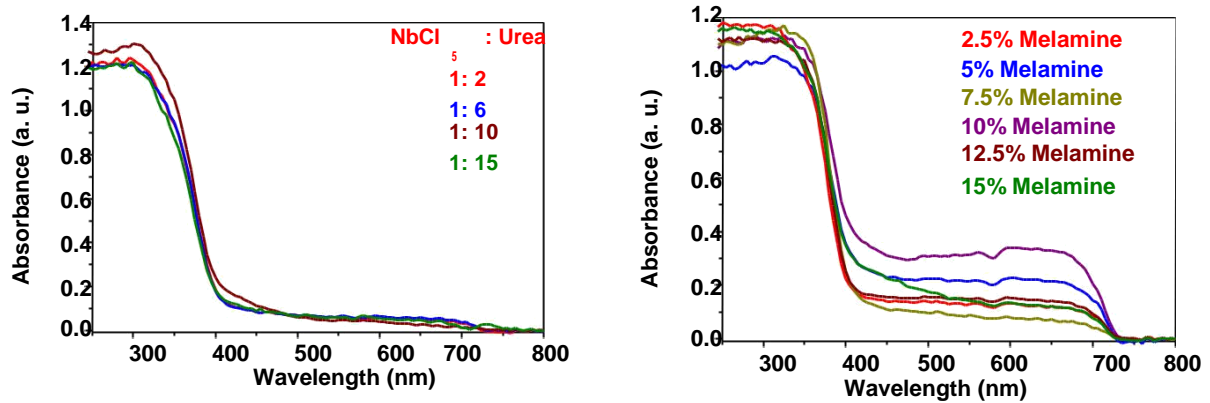


Figure 3.3 Diffuse reflectance UV-Visible absorbance spectra of Sol-Gel process and Solid-solid combustion process

The as synthesized Nb_2O_5 showed the single broad absorption peak. There is shift in peaks as the concentration of melamine is changed. The maximum shift is observed for 10% melamine addition whereas the shift in peaks is less for solid-solid combustion process as compared to sol-gel process. This indicates the change in band gap structure thus leads proves nitrogen doping in some cases where there is shift.

3.4. Electrochemical Characterization

The capacitive properties of the Nitrogen-doped Nb₂O₅ are tested via three electrode system. In each experiment a symmetric arrangement is utilized, ensuring both working and counter electrode are of the same composition. The electrodes are connected and emersed into the electrolyte of 1M Na₂SO₄. The capacitive performance is evaluated by means of Galvanostatic charge discharge cycle and cyclic voltammetry. And internal resistance test performed using electrochemical impedance spectroscopy. The system is fixed at -0.8V to -0.3V (for sol-gel process) and -1.25V to -0.5V (solid combustion process) potential window for CV and GCD.

(a) Sol- Gel Method

1. N-Nb₂O₅ (2.5% melamine)

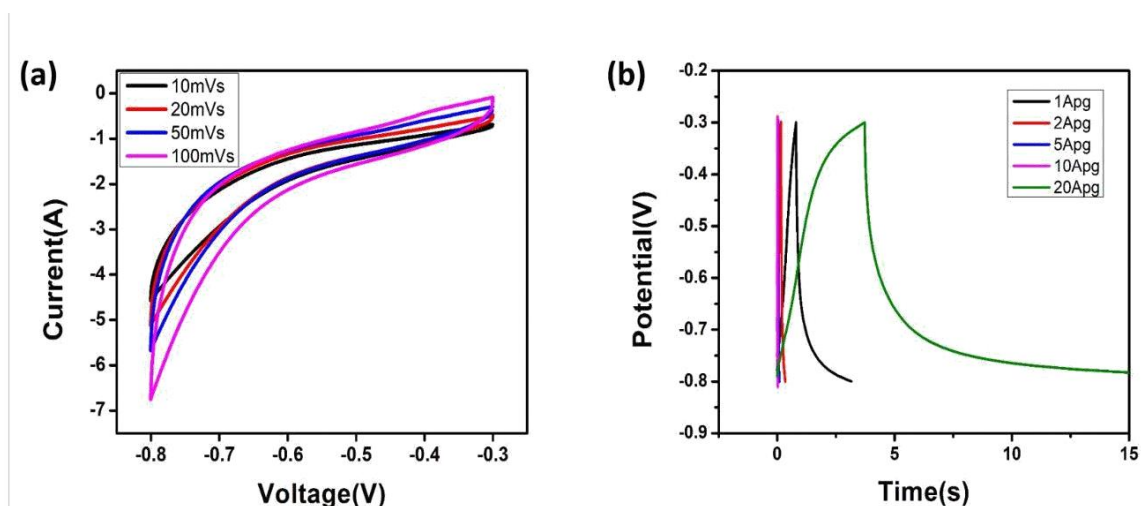


Fig3.4.1 N-Nb₂O₅ curves (a) CV at various scan rate (b) CD at various current density

2. N-Nb₂O₅ (5% melamine)

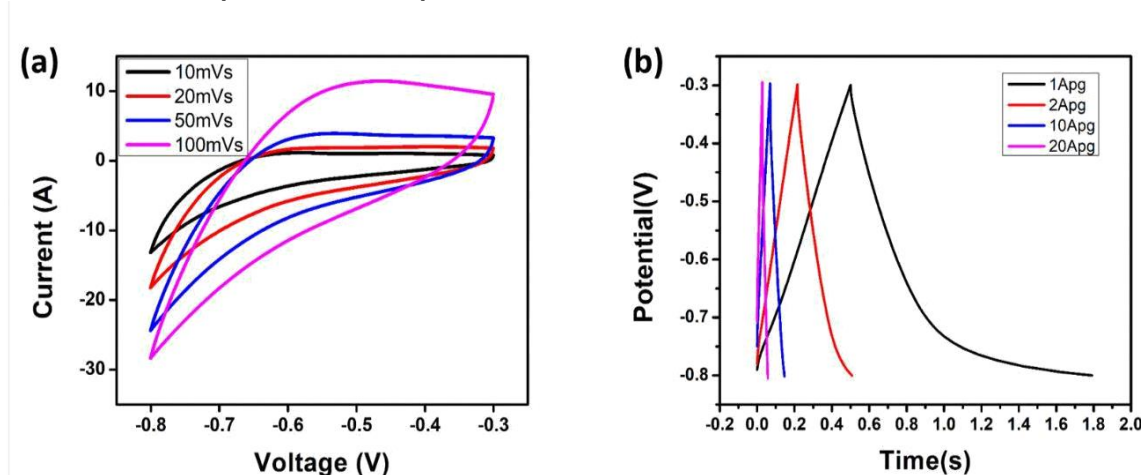


Fig3.4.2 N-Nb₂O₅ curves (a) CV at various scan rate (b) CD at various current density

3. N-Nb₂O₅ (7.5% melamine)

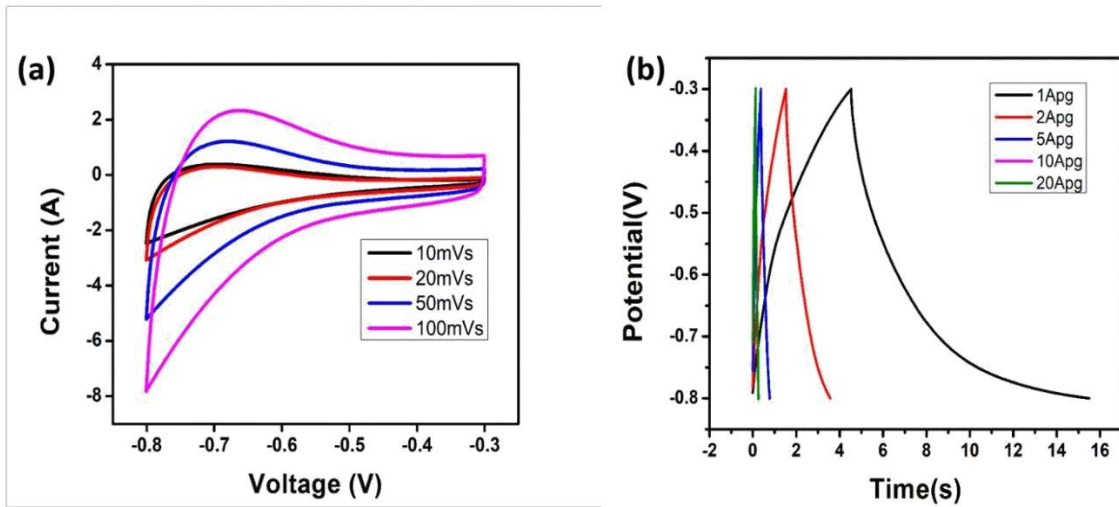


Fig3.4.3 N-Nb₂O₅ curves (a) CV at various scan rate (b) CD at various current density

4. N-Nb₂O₅ (10% melamine)

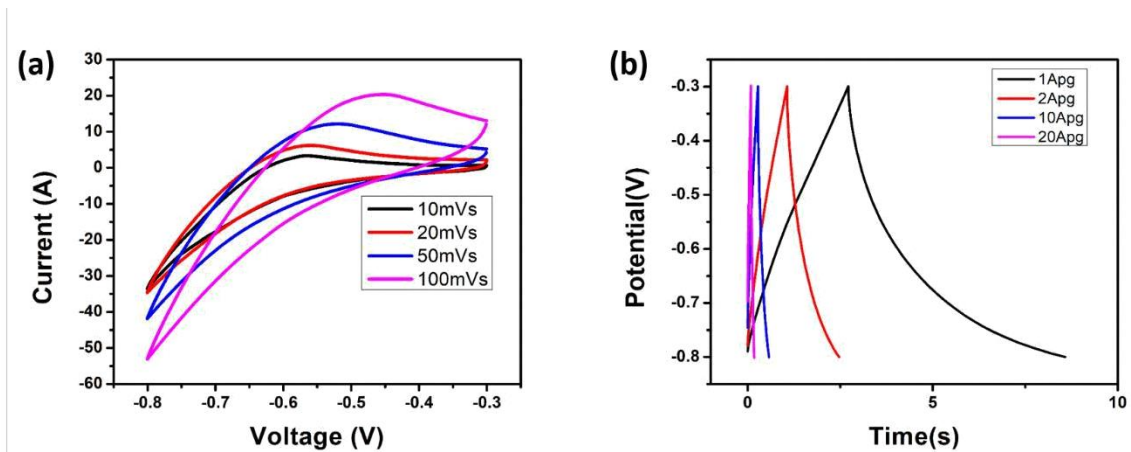


Fig3.4.4 N-Nb₂O₅ curves (a) CV at various scan rate (b) CD at various current density

5. N-Nb₂O₅ (15% melamine)

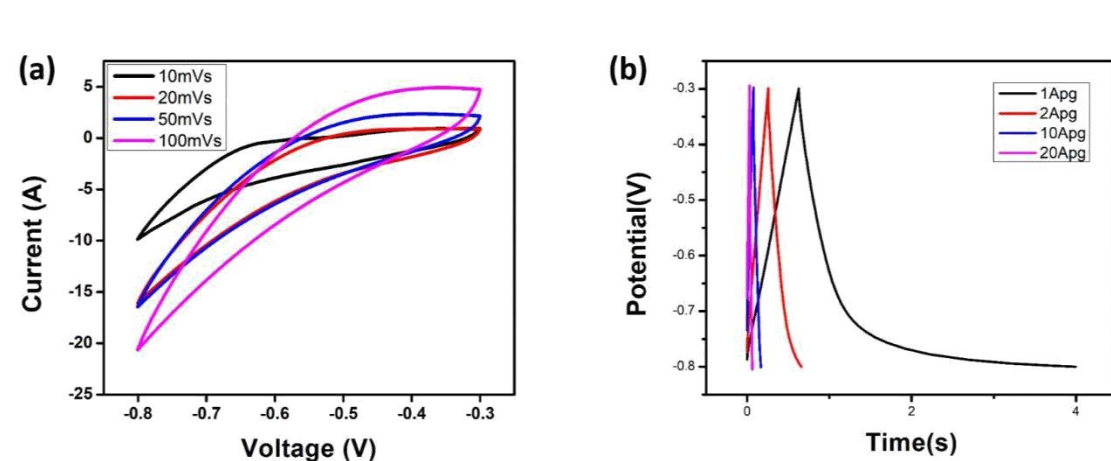


Fig3.4.5 N-Nb₂O₅ curves (a) CV at various scan rate (b) CD at various current density

Electrochemical behaviour of the synthesized N-doped Nb₂O₅ by sol-gel process was first evaluated by CV experiments. The CV was gathered at scan rates ranging from 10 to 100 mV s⁻¹ for different melamine concentration, which implies that this electrode material shows better capacitive performance. At the scan rate of 10 mV s⁻¹, the specific capacitances of 22 Fg⁻¹, 191 Fg⁻¹, 51.8 Fg⁻¹, 410 Fg⁻¹, 190.62 Fg⁻¹ were achieved for N-doped Nb₂O₅ for 2.5%,5%,7.5%,10%,15% melamine concentration electrodes, respectively. Finally we can observe the capacitance drop for nitrogen doped Nb₂O₅ electrodes we increase the scan rate. We can observe that for lower scan rates allow to diffuse nitrogen into the pores inside electrode material which provides more surface available for the reaction. But if we increase the scan rate, This gets limited to outer surface of the electrode material. Observing this we can state that the specific capacitance values decrease by increasing the scan rate as observed above in the plots.^[27] Further, it has been demonstrated the maximum capacitance is observed for 10% melamine, this is due to the nitrogen to oxygen ratio for 10% melamine solution. From the above CV profiles we can conclude that the specific Capacitance increases from 2.5% to 5% to 10% and decreases for 7.5% and 15%. This irregular trend can be due to the nitrogen to oxygen ratio and fading of nitrogen over the time leaving behind the cavities, thus leading to change in surface area. As seen in Fig3.4.6 there is difference in specific capacitance obtained from charge discharge profile and CV profile. This huge difference has to be evaluated further through experimentation.

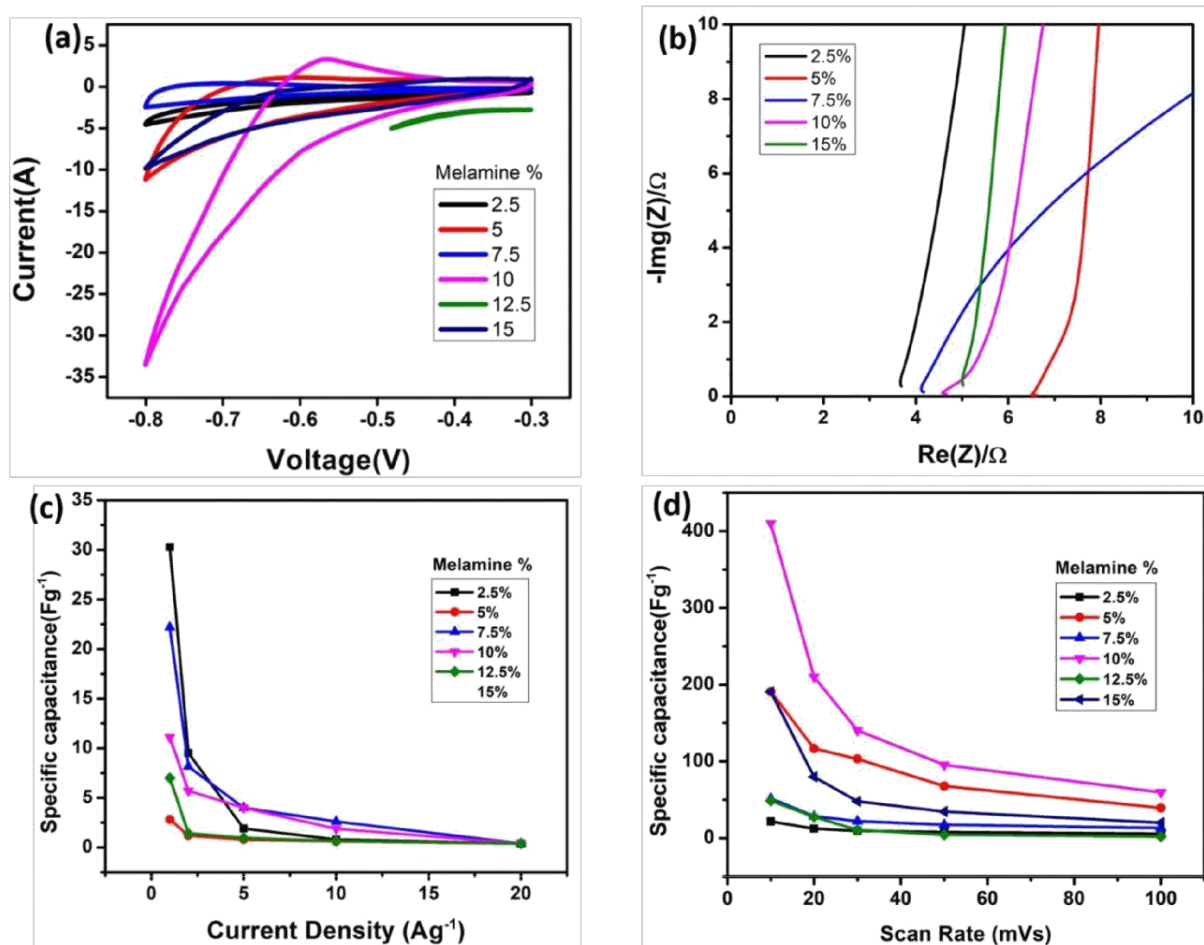


Fig 3.4.6 N-Nb₂O₅ curves at different percentage (a) CV at 10 mVs (b) Nyquist Plot (c) Rate Capability (d) Specific Capacitance Vs Scan rate For the Synthesized N- Nb₂O₅

The ion diffusion rates and internal resistance of the synthesized electrode materials was observed by using EIS. The impedance curve, known as Nyquist plots, of the electrodes are shown in Fig. 3.4.6. A typical supercapacitor's Nyquist plot shows a linear part over high and low frequency regions and a semi circular pattern. As we can see in Fig. 3.4.6, all the electrodes show which comparatively low charge transfer resistance (R_{ct}) due to smaller semi circular pattern which can be due to interaction between active electrode and ions of electrolyte in high frequency range.^[26] This studies show that N-doped Nb₂O₅ electrodes have fairly good R_{ct} values and can be used for conductivities in supercapacitors. The Nyquist plots for the electrodes shows vertical lines in low-frequency range ^[27]. EIS measurements were conducted at the frequency range from 50mHz to 100kHz .

(b) Solid- Solid method

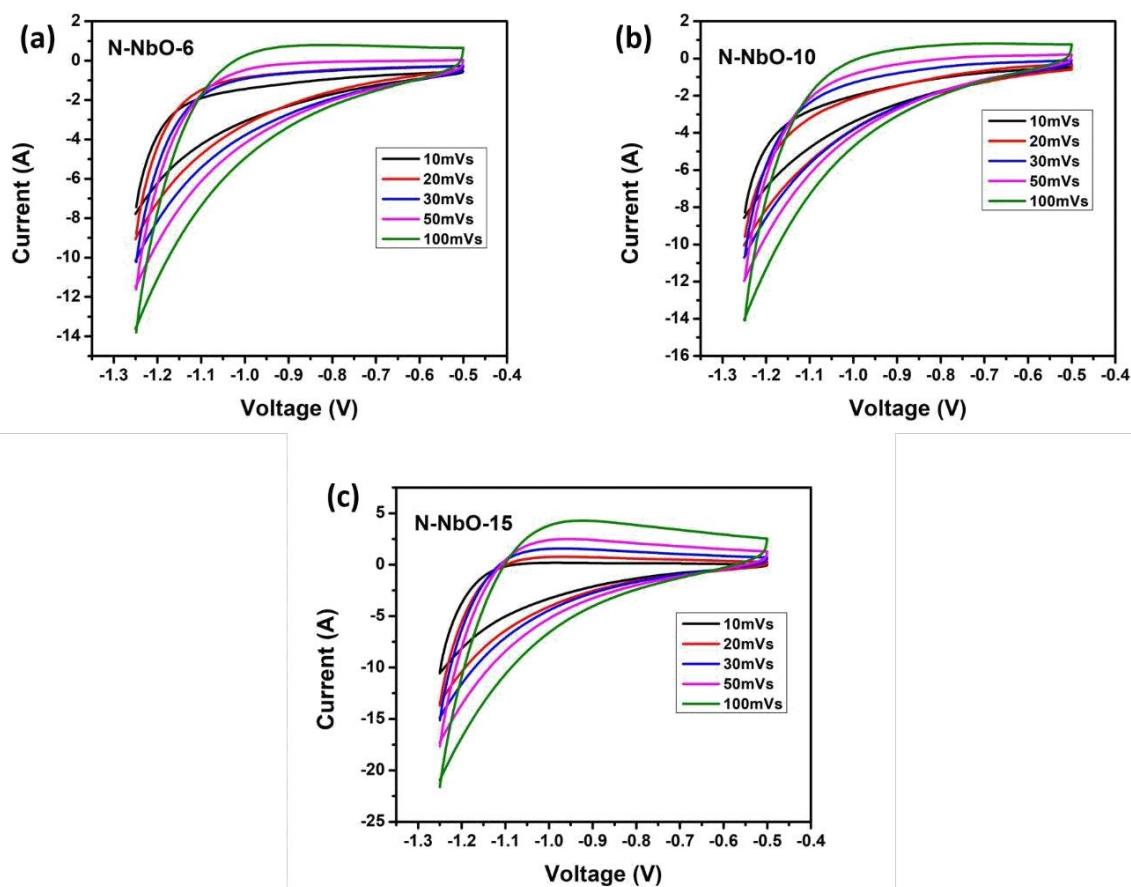


Fig3.4.7 CV curves at different scan rate for (a) N-NbO-6, (b) N-NbO-10 and (c) N-NbO-15

Electrochemical behaviour of the synthesized N-doped Nb_2O_5 by solid combustion technique was first evaluated by CV experiments. The CV was gathered at scan rates ranging from 10 to 100 mV s^{-1} for different urea concentration, which implies that this electrode material shows better capacitive performance. At the scan rate of 10 mV s^{-1} , the specific capacitances of 47.44 Fg^{-1} , 47.93 Fg^{-1} , 90.65 Fg^{-1} , were achieved for N-NbO-6 N-NbO-10, N-NbO-15 electrodes, respectively Finally we can observe the capacitance drop for nitrogen doped Nb_2O_5 electrodes we increase the scan rate. We can observe that for lower scan rates allow to diffuse nitrogen into the pores inside electrode material which provides more surface available for the reaction . But if we increase the scan rate , This gets limited to outer surface of the electrode material. Observing this we can state that the specific capacitance values decrease by increasing the scan rate as observed above in the plots.^[27]

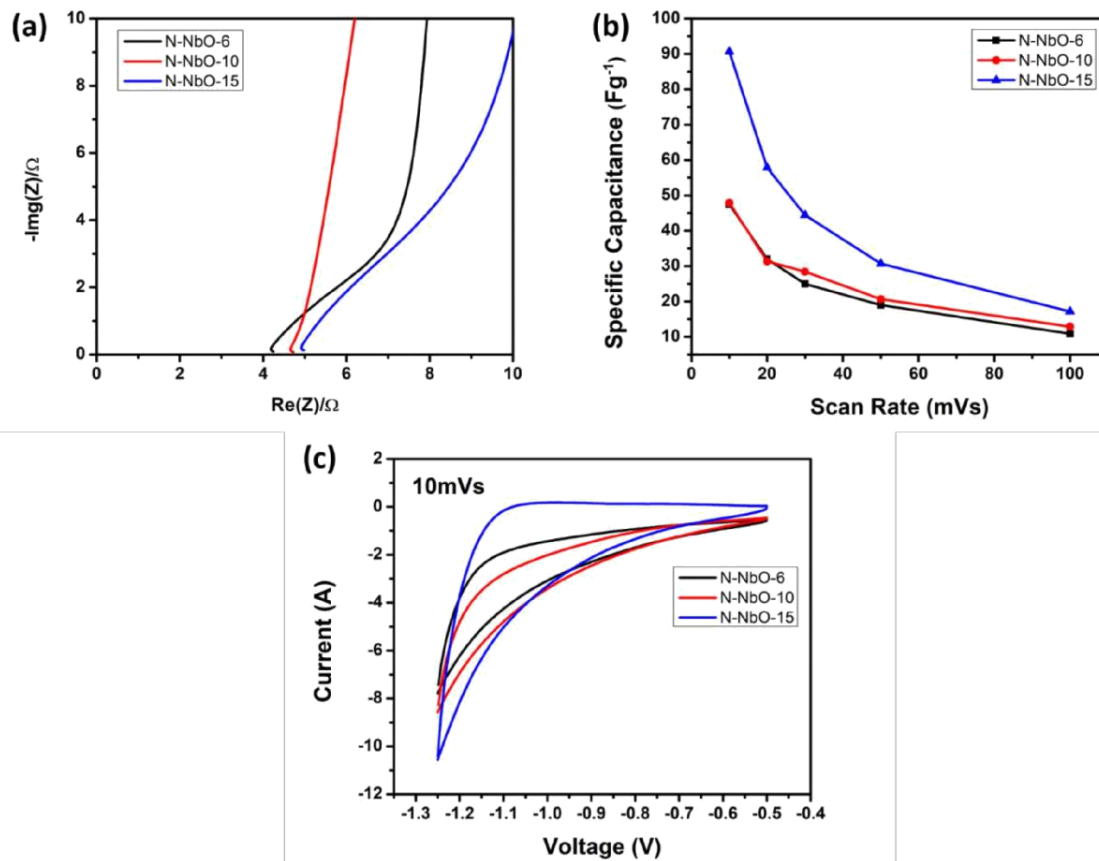


Fig 3.4.8 Nitrogen doped Nb_2O_5 (a) Nyquist plot (b) Specific capacitance vs scan rate (c) CV at 10mVs

Moreover, it has been observed the maximum capacitance is observed for N-NbO-15, this is due to the nitrogen to oxygen ratio for N-NbO-15. From the above CV profiles we can conclude that the specific Capacitance increases for N-NbO-6, N-NbO-10, N-NbO-15 electrodes as seen in fig.3.4.8 due to increase in urea concentration. A typical supercapacitor's Nyquist plot shows a linear part over high and low frequency regions and a semi-circular pattern.. As shown in Fig. 3.4.8, all electrodes show that N-doped Nb_2O_5 electrodes have fairly good Rct values and can be used for conductivities in supercapacitors. The Nyquist plot for the electrodes shows vertical lines in low-frequency range [27]. EIS measurements were conducted at the frequency range from 50mHz to 100kHz

CONCLUSIONS AND FUTURE OUTLOOK

Doping of Nb_2O_5 with nitrogen through Solid combustion and sol-gel method has enhanced the supercapacitive performance of the Nb_2O_5 material by changing the concentration and source of nitrogen. The Nitrogen doping did not show any change in crystal structure in both the processes. At the same time morphological study shows the reduction in the size of nano particles for adequate amount of nitrogen. Excess of nitrogen doping shows clusters of particles which in turn show lower activity.

The optical properties of N doped Nb_2O_5 clearly shows the narrowing in the band gap for both the processes. It clearly shows the doping of nitrogen in Nb_2O_5 .

Electrochemical characterizations of the synthesized materials have confirmed that the N-doped Nb_2O_5 shows comparatively better supercapacitive performance for Sol-gel process compared to the N-doped Nb_2O_5 through Solid combustion process. The notable increment in the supercapacitive performance in the case of N-doped Nb_2O_5 Can be due to the improved conductivity of Nb_2O_5 by better doping of nitrogen atoms in Sol-gel process.

The doping of nitrogen through sol-gel process shows irregular trend whereas doping of nitrogen through solid combustion shows increase in specific capacitance as we increase the concentration of urea, there is huge difference in specific capacitance obtained from CV and CD curves for both sol-gel and solid combustion process which has to be examined detail through further experimentation As a result, we can say doping of nitrogen into the crystal structure of Nb_2O_5 is a suitable process to some extent to enhance the properties in terms of supercapacitance of the Nb_2O_5 .

REFERENCES

1. S.M.Xu, C.M.Hessel, H.Ren, R.B.Yu, Q.Jin, M.Yang, H.J.Zhao and D.Wang, α -Fe₂O₃ multi-shelled hollow microspheres for lithium ion battery anodes with superior capacity and charge retention, *Energy Environ. Sci.* 7 (2014) 632-637.
2. Anirudha K. Kulkarni, C. S. Praveen, Yogesh A. Sethi, Rajendra Popat Panmand et al. "Nanostructured N doped orthorhombic Nb₂O₅ as an efficient stable photocatalyst for hydrogen generation under visible light", *Dalton Trans.*, 2017.
3. Amin Hodaei, Amin Shiralizadeh Dezfuli, Hamid Reza Naderi. "A high-performance supercapacitor based on N-doped TiO₂ nanoparticles", *Journal of Materials Science: Materials in Electronics*, 2018.
4. P. Yang, W. Mai, Flexible solid-state electrochemical supercapacitors, *Nano Energy* 8 (2014) 274-290.
5. W. Guo, C. Xu, X. Wang, S. Wang, C. Pan, C. Lin and Z. Wang, Rectangular Bunched Rutile TiO₂ Nanorod Arrays Grown on Carbon Fiber for Dye-Sensitized Solar Cells, *J. Am. Chem. Soc.* 134 (2012) 4437-4441
6. Wang YD, Yang LF, Zhou ZL, Li YF, Wu XH. Effects of calcining temperature on lattice constants and gas-sensing properties of Nb₂O₅. *Materials Letters*. 2001;49(5):277-281.
7. Chandran, P.; Ghosh, A.; Ramaprabhu, S. High-Performance Platinum-Free Oxygen Reduction Reaction and Hydrogen Oxidation Reaction Catalyst in Polymer Electrolyte Membrane Fuel Cell. *Sci. Rep.* **2018**, 8 (1), 3591.
8. Characteristics, C. Chapter 2 Electrode / Electrolyte Interfaces: Structure and. 1900.
9. Principle, T. W.; Cell, S. The Working Principle of a Solar Cell. **1921**, 1, 21–24.
10. <https://www.explainthatstuff.com/how-supercapacitors-work.html>
11. Principle, T. W.; Cell, S. The Working Principle of a Solar Cell. **1921**, 1, 21–24.
12. Characteristics, C. Chapter 2 Electrode / Electrolyte Interfaces: Structure and. **1900**.
13. Arkady A. Karyakin, Prussian blue and Its Analogues: Electrochemistry and Analytical Applications, *Electroanalysis* 13 (10) (1001) 813-819.
14. Enrique Herrero, Lisa J. Buller, Héctor D. Abruña, Underpotential Deposition at Single Crystal Surfaces of Au, Pt, Ag and Other Materials, *Chem. Rev.* 101 (7) (1001) 1897–1930.

- 15 Jiang, J., Zhang, Y., Nie, P., Xu, G., Shi, M., Wang, J., & Zhang, X. (2018). Progress of nanostructured electrode materials for supercapacitors. *Advanced Sustainable Systems*, 2(1), 1700110.
- 16 Veronica Augustyn, Patrice Simon, Bruce Dunn, Pseudocapacitive Oxide Materials for High-rate Electrochemical Energy Storage, *Energy Environ. Sci.* 7 (5) (2014) 1597-1614.
- 17 Venkataraman, A. (2015). Pseudocapacitors for Energy Storage.
- 18 Simon, P., & Gogotsi, Y. (2010). Materials for electrochemical capacitors. In *Nanoscience and Technology: A Collection of Reviews from Nature Journals* (pp. 320-329).
- 19 Mujawar SH, Inamdar AI, Patil SB, Patil PS. Electrochromic properties of spray-deposited niobium oxide thin films. *Solid State Ionics*. 2006;177(37-38):3333-3338.
- 20 Jose R, Thavasi V, Ramakhrisna S. Metal Oxides for DyeSensitized Solar Cells. *Journal of the American Ceramic Society*. 2009;92(2):289-301.
- 21 Lira-Cantu M, Krebs FC. Hybrid solar cells based on MEHPPV and thin film semiconductor oxides (TiO₂ , Nb₂ O₅ , ZnO, CeO₂ and CeO₂ –CTiO₂): Performance improvement during long-time irradiation. *Solar Energy Materials and Solar Cells*. 2006; 90(14):2076-2086.
- 22 Ahn KS, Kang MS, Lee JK, Shin BC, Lee JW. Enhanced electron diffusion length of mesoporous TiO₂ film by using Nb₂O₅ energy barrier for dye-sensitized solar cells. *Applied Physics Letters*. 2006;89:013103.
23. Hashemzadeh F, Gaffarimejad A, Rahimi R. Porous p-NiO/n-Nb₂O₅ nanocomposites prepared by an EISA route with enhanced photocatalytic activity in simultaneous Cr(VI) reduction and methyl orange decoloration under visible light irradiation. *Journal of Hazardous Materials*. 2015;286:64-74.
- 23 R. Marom, S.F. Amalraj, N. Leifer, D. Jacob, D. Aurbach, *J. Mater. Chem.* 21 (2011) 9938-9954.
- 24 Kulkarni S., *Nanotechnology: Principles and Practices*, Third Edition, Springer, 2015.
- 26.H. Kim, M.Y. Cho, M.H. Kim, K.Y. Park, H. Gwon, Y. Lee, K.C. Roh, K. Kang, A novel high-energy hybrid supercapacitor with an anatase TiO₂– reduced graphene oxide anode and an activated carbon cathode. *Adv. Energy Mater.* 3(11), 1500–1506 (2013)

27. V.H. Pham, T.-D. Nguyen-Phan, X. Tong, B. Rajagopalan, J.S. Chung, J.H. Dickerson, Hydrogenated TiO₂@ reduced graphene oxide sandwich-like nanosheets for high voltage supercapacitor applications. *Carbon* **126**, 135–144 (2018)